Internal energy of HCl upon photolysis of 2-chloropropene at 193 nm investigated with time-resolved Fourier-transform spectroscopy and quasiclassical trajectories

Chih-Min Chang, Yu-Hsuan Huang, Suet-Yi Liu, Yuan-Pern Lee, Marta Pombar-Pérez, Emilio Martínez-Núñez, and Saulo A. Vázquez

Citation: The Journal of Chemical Physics **129**, 224301 (2008); doi: 10.1063/1.3023149
View online: http://dx.doi.org/10.1063/1.3023149
View Table of Contents: http://scitation.aip.org/content/aip/journal/jcp/129/22?ver=pdfcov
Published by the AIP Publishing

Articles you may be interested in

Photolysis of n -butyl nitrite and isoamyl nitrite at 355 nm: A time-resolved Fourier transform infrared emission spectroscopy and ab initio study
J. Chem. Phys. **130**, 174314 (2009); 10.1063/1.3129806

Molecular elimination in photolysis of fluorobenzene at 193 nm: Internal energy of HF determined with time-resolved Fourier-transform spectroscopy
J. Chem. Phys. **121**, 8792 (2004); 10.1063/1.1802537

Three-center versus four-center elimination of haloethene: Internal energies of HCl and HF on photolysis of CF 2 CHCl at 193 nm determined with time-resolved Fourier-transform spectroscopy
J. Chem. Phys. **117**, 9785 (2002); 10.1063/1.1518028

I. Three-center versus four-center HCl-elimination in photolysis of vinyl chloride at 193 nm: Bimodal rotational distribution of HCl (v7) detected with time-resolved Fourier-transform spectroscopy
J. Chem. Phys. **114**, 160 (2001); 10.1063/1.1328736

Photodissociation of 1,1-difluoroethene (CH 2 CF 2) at 193 nm monitored with step-scan time-resolved Fourier-transform infrared emission spectroscopy
J. Chem. Phys. **111**, 9233 (1999); 10.1063/1.480029

This article is copyrighted as indicated in the article. Reuse of AIP content is subject to the terms at: http://scitation.aip.org/termsconditions. Downloaded to IP: 140.113.38.11 On: Wed, 30 Apr 2014 06:14:52

Internal energy of HCl upon photolysis of 2-chloropropene at 193 nm investigated with time-resolved Fourier-transform spectroscopy and quasiclassical trajectories

Chih-Min Chang,[1] Yu-Hsuan Huang,[1] Suet-Yi Liu,[1] Yuan-Pern Lee,[1,2,a)]
Marta Pombar-Pérez,[3] Emilio Martínez-Núñez,[3] and Saulo A. Vázquez[3,a)]
[1]*Department of Applied Chemistry, National Chiao Tung University, Hsinchu 30010, Taiwan*
[2]*Institute of Molecular Science, National Chiao Tung University, Hsinchu 30010, Taiwan and Institute of Atomic and Molecular Sciences, Academia Sinica, Taipei 10617, Taiwan*
[3]*Departamento de Química Física, Facultad de Química, Universidade de Santiago de Compostela 15782, Santiago de Compostela, Spain*

(Received 21 August 2008; accepted 22 October 2008; published online 8 December 2008)

Following photodissociation of 2-chloropropene ($H_2CCClCH_3$) at 193 nm, vibration-rotationally resolved emission spectra of HCl ($v \leq 6$) in the spectral region of 1900–2900 cm^{-1} were recorded with a step-scan time-resolved Fourier-transform spectrometer. All vibrational levels show a small low-J component corresponding to ~400 K and a major high-J component corresponding to 7100–18 700 K with average rotational energy of $39 \pm {}^{11}_{3}$ kJ mol^{-1}. The vibrational population of HCl is inverted at $v=2$, and the average vibrational energy is 86 ± 5 kJ mol^{-1}. Two possible channels of molecular elimination producing HCl+propyne or HCl+allene cannot be distinguished positively based on the observed internal energy distribution of HCl. The observed rotational distributions fit qualitatively with the distributions of both channels obtained with quasiclassical trajectories (QCTs), but the QCT calculations predict negligible populations for states at small J. The observed vibrational distribution agrees satisfactorily with the total QCT distribution obtained as a weighted sum of contributions from both four-center elimination channels. Internal energy distributions of HCl from 2-chloropropene and vinyl chloride are compared. © *2008 American Institute of Physics*. [DOI: 10.1063/1.3023149]

I. INTRODUCTION

The photolysis of vinyl halides (CH_2CHX, X=F, Cl, or Br) and their derivatives is of interest to many researchers partly because this reaction proceeds on multiple potential-energy surfaces associated with channels for simple bond scission and molecular elimination.[1,2] Experiments with photofragment translational spectroscopy provides detailed dynamics of most dissociation channels,[3] but these channels become indistinguishable when the fragments produced via two different paths possess similar distributions of translational energy. For example, the translational energy distribution of HCl produced upon photolysis of vinyl chloride at 193 nm provides little information about its origin from either a three-center or a four-center molecular elimination.[3]

Step-scan time-resolved Fourier-transform spectroscopy (TR-FTS) has been demonstrated to provide certain advantages over other techniques involving resonance-enhanced multiphoton ionization or laser-induced fluorescence in determining the distributions of internal energy of reaction products;[1,2,4–6] its capability to detect emission over a wide spectral range with sufficient spectral and temporal resolution might yield information superior to that from other methods. Following photodissociation of vinyl chloride at 193 nm, we observed vibration-rotationally resolved emission spectra of HCl ($v \leq 7$) with TR-FTS.[1,7] Further work extended to photolysis of vinyl fluoride and vinyl bromide[2] indicated that the HX (X=F, Cl, or Br) products observed in all vibrational levels show bimodal rotational distributions for which we proposed that the high-J component is associated with production via three-center (α,α) molecular elimination and the low-J component with four-center (α,β) elimination. Martínez-Núñez *et al.*[8,9] employed quasiclassical trajectory (QCT) calculations to investigate energy partitions of HCl upon photodissociation of CH_2CHCl at 193 nm and reported that three-center elimination and isomerization of vinylidene to acetylene take place in a concerted, nonsynchronous fashion. In agreement with previous experimental results,[1,7] the four-center elimination produces much vibrationally excited HCl, with a population inversion predicted at $v=1$ (Ref. 9) or $v=3$ (Ref. 8). The predicted overall rotational distributions from both HCl-elimination channels also agree satisfactorily with those of previous experiments using supersonic jets;[7] results from experiments with a flow system show some rotational quenching that yields a slightly enhanced fraction of the low-J component. Martínez-Núñez *et al.*[8,9] predicted, however, that HCl produced from four-center elimination is more rotationally excited than that from three-center elimination, in contrast with the revised-impulse model that predicts little rotational excitation for four-center elimination but extensive rotational excitation for three-

a)Authors to whom correspondence should be addressed. Electronic addresses: yplee@mail.nctu.edu.tw and saulo.vazquez@usc.es.

 © 2008 American Institute of Physics

This article is copyrighted as indicated in the article. Reuse of AIP content is subject to the terms at: http://scitation.aip.org/termsconditions. Downloaded to IP: 140.113.38.11 On: Wed, 30 Apr 2014 06:14:52

center elimination.[1] An understanding of the dynamics of reactions of this type requires further investigations.

2-chloropropene ($H_2CCClCH_3$) has a structure similar to vinyl chloride except that the α-H is replaced by a methyl group. In addition to the bond scission channels, HCl elimination is expected to proceed via the four-center channel involving the C=C bond without interference from the three-center elimination. If the conclusion derived with QCTs for photolysis of vinyl halides are also valid for 2-chloropropene, we expect to observe HCl highly rotationally and vibrationally excited. Comparison of experimental and calculated results on the distribution of internal states of HCl thus provides further tests to assist an understanding of the photodissociation dynamics of molecular elimination channels of vinyl halide derivatives.

Investigating the photodissociation of 2-chloropropene at 193 nm, Mueller *et al.*[10] recorded photofragment translational spectra and observed three significant primary channels with branching ratios of 0.62:0.23:0.15: a channel for excited-state C–Cl scission producing rapid Cl, a channel for ground-state C–Cl scission producing slow Cl, and a channel for elimination of HCl; a minor channel for $C-CH_3$ scission was also observed. According to quantum-chemical calculations, the elimination of HCl might proceed via two channels: four-center elimination involving the C=C bond to form HCl and propyne ($HC\equiv CCH_3$) and another four-center elimination involving the C–C bond to form HCl and allene ($H_2C=C=CH_2$),[11]

$$H_2CCClCH_3 + h\nu \rightarrow HCl + HC\equiv CCH_3, \quad \Delta H = 105 \text{ kJ mol}^{-1}, \tag{1}$$

$$H_2CCClCH_3 + h\nu \rightarrow HCl + H_2C=C=CH_2, \quad \Delta H = 109 \text{ kJ mol}^{-1}. \tag{2}$$

The calculated barrier heights of these two channels are nearly identical, with 280 and 282 kJ mol^{-1} for reactions (1) and (2), respectively, at the G3//B3LYP level of theory. According to the Rice–Ramsperger–Kassel–Marcus (RRKM) calculations, the branching ratio of reactions (1) and (2) is about 0.63:0.37 for excitation energy near 624 kJ mol^{-1},[10] corresponding to a photon energy at 193.3 nm plus the internal energy of 2-chloropropene. The time-of-flight spectra of HCl reported by Mueller *et al.*[10] using photofragment translational spectroscopy show smooth profiles without an obvious indication of the presence of two distinct molecular elimination channels; the corresponding kinetic-energy distribution peaks near 33 kJ mol^{-1} and extends to ~250 kJ mol^{-1}.

We report here investigation of the HCl-elimination channels upon photolysis of 2-chloropropene at 193 nm with TR-FTS and QCT calculations. We compare the observed distribution of internal energy of HCl with four-center HCl elimination of vinyl chloride. In both cases, vibrational inversion and extensive rotational excitation of HCl were observed, consistent with the results of trajectory calculations.

II. EXPERIMENTS

The apparatus employed to obtain step-scan time-resolved Fourier-transform spectra has been described previously;[4,12,13] only a brief summary is given here. A pulsed slit nozzle (General Valve, length of 1.25 cm and width of 125 μm) heated to ~80 °C was placed in front of light-collecting Welsh mirrors; their opening periods were controlled with a pulse generator (General Valve, IOTA). The vacuum chamber was pumped with a 16 in. diffusion pump (10 000 l s^{-1}) backed with a dry pump (Taiko, 25 000 l min^{-1}). The pressure of the system was maintained typically under 6×10^{-5} Torr when the slit was opened for 350–370 μs at 23 Hz; the stagnation pressure was 380 Torr and the concentration of 2-chloropropene in He was about 15%. A lens mildly focused the photolysis beam from an ArF laser at 193 nm (Gam Laser, EX100H/60) to ~40 mm^2 with a fluence of 50–60 mJ cm^{-2} across the jet about 16–20 mm above the nozzle. A linear dependence of the IR emission signal on the fluence of the photolysis laser was observed below 60 mJ cm^{-2}. The absorption cross section of 2-chloropropene at 193 nm is 5.1×10^{-18} cm^2; ~27% of 2-chloropropene was hence photodissociated. A filter either passing 200–2900 or 1670–2325 cm^{-1} was employed and an InSb detector with a rise time of 0.22 μs; its transient signal was amplified with an effective bandwidth of 1 MHz before being digitized with an external data-acquisition board (PAD1232, 12 bit analog to digital converter) at 25 ns resolution. Data were typically averaged over 75 laser pulses at each scan step; 4665 scan steps were performed to yield an interferogram resulting in a spectrum of resolution of 0.4 cm^{-1} for HCl. To improve the ratio of signal to noise (S/N) of the spectrum, every 80 time-resolved spectra were subsequently summed to yield a satisfactory spectrum representing emission at 2 μs intervals after photolysis. Four such spectra recorded under similar conditions were averaged to improve further the ratio of S/N.

2-chloropropene (Aldrich, 98%) was used without purification except for degassing; no impurity was detected in IR spectra.

III. THEORETICAL METHOD

Trajectories were initiated at the transition states using a microcanonical, quasiclassical normal-mode sampling[14,15] and at an excitation energy equivalent to a laser wavelength of 193 nm. The trajectories were propagated "on the fly," that is, with energies and forces taken directly from electronic structure calculations. Following the strategy utilized in previous QCT calculations on related systems,[8,16–18] we employed semiempirical AM1 Hamiltonians with specific reaction parameters (AM1-SRP), obtained by fits to benchmark *ab initio* data. Transition state structures were also optimized with the B3LYP/6-311G++(d,p) density-functional theory[19,20] using the GAUSSIAN 03 program for comparison.[21]

The classical equations of motion were integrated with a fixed step size of 0.05 fs using the Adams–Moulton algorithm implemented in a code that interfaces the classical trajectory program GENDYN (Ref. 22) with the semiempirical package MOPAC7.0.[23] The trajectories were halted and the

This article is copyrighted as indicated in the article. Reuse of AIP content is subject to the terms at: http://scitation.aip.org/termsconditions. Downloaded to IP: 140.113.38.11 On: Wed, 30 Apr 2014 06:14:52

product energies were computed when the separation between the centers of mass of the photofragments attained 10 Å. The rotational and vibrational quantum numbers of HCl were evaluated with the Einstein–Brillouin–Keller quantization of the action integral.[24–26] Ensembles of 10 000 trajectories were considered to provide good statistics. The total angular momentum was restricted to zero in these calculations.

IV. RESULTS

According to our previous experience of the photolysis of vinyl halides, even when the pressure of the system was decreased as much as practicable (~0.2 Torr) while maintaining a satisfactory S/N ratio, slight rotational quenching still occurred within 1 μs period after photolysis.[1,7] Previous experiments with vinyl chloride seeded in a supersonic jet eliminate this quenching problem and yielded a nascent distribution of internal states of fragments upon photoirradiation.[7] For this reason we here describe experimental results obtained only upon photolysis of 2-chloropropene expanded through a supersonic slit jet.

A. Emission of HCl

Figure 1 shows a spectrum of HCl emission at 0.4 cm^{-1} resolution recorded 0.0–2.0 μs after photolysis of 2-chloropropene seeded in a He supersonic jet. The spectrum clearly exhibits extensive rotational excitation of HCl with obvious *R* band heads for $v'=4$ and 5. Lines associated with J' up to 34 (for $v'=1$) and v' up to 6 were observed. Rotational distributions for each vibrational level, assigned based on spectral parameters reported by Arunan *et al.*[27] and Coxon and Roychowdhury,[28] are shown as stick diagrams; lines marked with "×" indicate overlapped lines. The simulated spectrum is shown as downward peaks at the bottom of Fig. 1 for comparison. Each vibration-rotational line in the *P* branch was normalized with the instrument-response function and divided by its respective Einstein coefficient[29] to yield a relative population $P_v(J')$. Partially overlapped lines were deconvoluted to yield their intensities. Semilogarithmic plots of $P_v(J)/(2J+1)$ versus $J(J+1)$ for HCl $(1 \le v \le 6)$ produced from 2-chloropropene (symbol "○") are shown in Fig. 2. Error limits for each $P_v(J)$ were typically derived by taking into account the errors in the determination of the baselines; for overlapped lines, additional errors resulted from curve fitting were also taken into account.

The rotational distribution of HCl is non-Boltzmann. These bimodal-like rotational distributions observed for all vibrational levels are fitted with biexponential functions to yield two rotational temperatures, as listed in Fig. 2; unless specified, error limits listed in this paper represent one standard deviation in fitting. We denote these two components as high-*J* and low-*J* components. Fitted Boltzmann-type rotational distributions for the high-*J* component of HCl yielded rotational temperatures of 7100–18 700 K for $v=1$–6. The contribution of the low-*J* component is small (<7%), with estimated rotational temperatures in the range of 130–420 K. Although care has been taken to avoid possible quenching of products in the supersonic jet, we cannot eliminate definitively the possibility that this low-*J* component is due to slight rotational quenching of HCl. However, as discussed in the following section, the small contribution of this low-*J* component does not affect the results significantly.

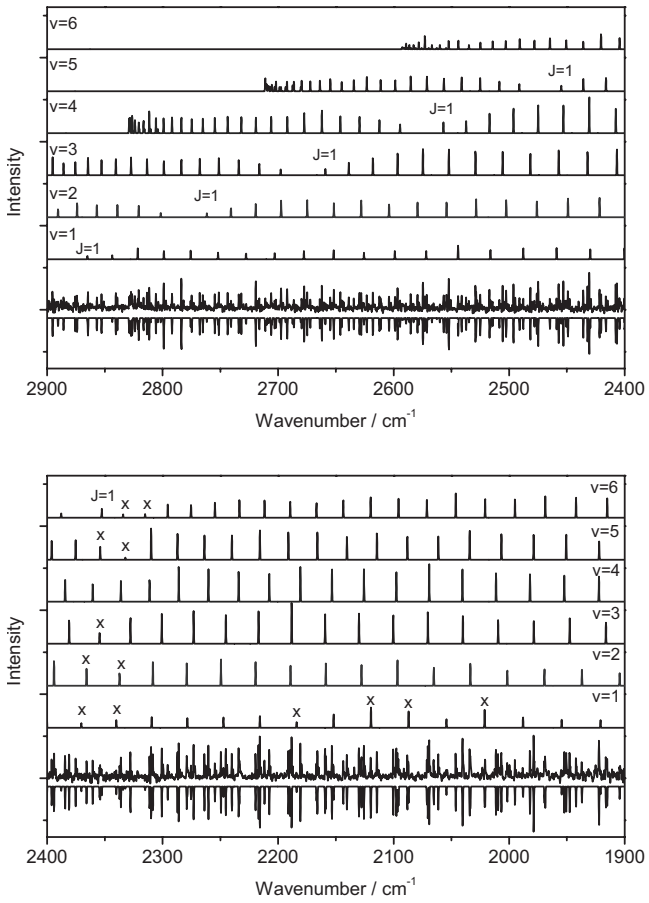

FIG. 1. Infrared emission spectra of HCl in spectral region of 1900–2900 cm^{-1} recorded 0.0–2.0 μs after photolysis of $H_2CCClCH_3$ seeded in He (stagnation pressure of 380 Torr) at 193 nm. Spectral resolution is 0.4 cm^{-1}; 75 laser pulses were averaged at each scan step. Four spectra recorded under similar conditions were averaged. Assignments are shown with stick diagrams at the top; a simulated overall spectrum is shown as downward peaks at the bottom. "*x*" indicates overlapped bands.

We assume a Boltzmann distribution for both high-*J* and low-*J* components and associate an interpolated population with overlapped lines and missing lines. Relative populations obtained on counting levels up to observed maximal *J* values in each vibrational level are listed as $\Sigma_J P_v(J)$ in Table I. We normalized values of $\Sigma_J P_v(J)$ associated with each vibrational state to yield a relative vibrational population, $(v=1):(v=2):(v=3):(v=4):(v=5):(v=6)=19.1\pm5.1:21.6\pm6.2:21.3\pm4.2:18.1\pm3.1:12.7\pm2.7:7.3\pm1.4$, showing an inversion of vibrational population at $v=2$ or 3; the error limits reflect the error in vibrational-rotational populations. Rotational energies for each vibrational level, $E_r(v)$, obtained on summing a product of rotational level energy and normalized population for each rotational level, are also listed in Table I. An average rotational energy of $E_r=39.4$ kJ mol^{-1} for the high-*J* component of HCl $(v=1-6)$ is derived on summing a product of vibrational population and associated $E_r(v)$.

The highest level of HCl observed, $J'=19$ of $v'=6$, has an energy of 18 977 cm^{-1} above the ground vibrational

This article is copyrighted as indicated in the article. Reuse of AIP content is subject to the terms at: http://scitation.aip.org/termsconditions. Downloaded to IP: 140.113.38.11 On: Wed, 30 Apr 2014 06:14:52

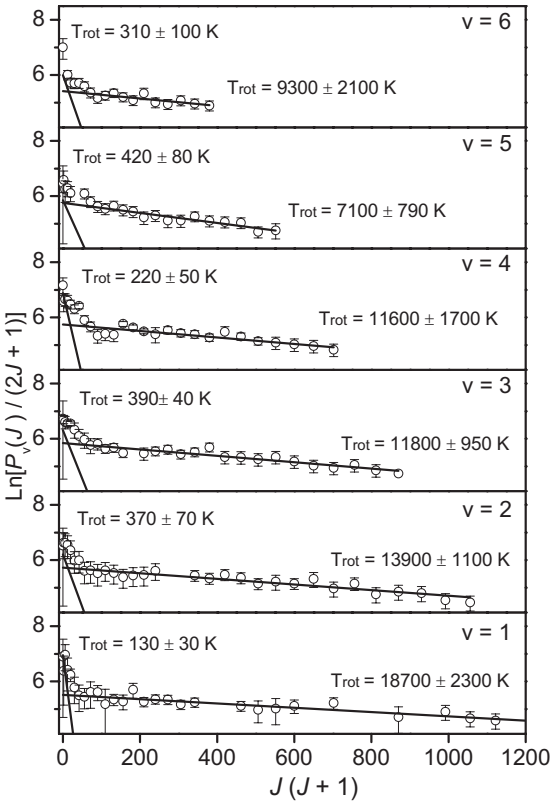

FIG. 2. Semilogarithmic plots of relative rotational populations of HCl ($v=1-6$, symbol ○) upon photolysis of $H_2CCClCH_3$ seeded in He (stagnation pressure of 380 Torr) at 193 nm. Solid lines represent least-squares fits of bimodal distributions.

level; this energy corresponds to $J_{max}(v)=41$, 37, 33, 29, and 24 for $v=1-5$, respectively. If we assume a Boltzmann distribution and associate an extrapolated population with unobserved lines up to $J_{max}(v)$ for each vibrational level to derive a revised population distribution, referred to as "extrapolated data," an average rotational energy of 50.1 kJ mol^{-1} is thus derived from extrapolated data. Taking this upper limit into account, we report an average rotational energy of HCl as 39^{+11}_{-3} kJ mol^{-1}.

Using a surprisal analysis, we estimated the population

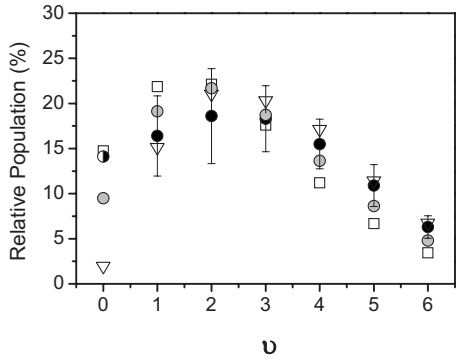

FIG. 3. Comparison of experimental and calculated vibrational distributions of HCl. Solid circle (with error bars): experimental data upon photolysis of $H_2CCClCH_3$ seeded in He (stagnation pressure 380 of Torr) at 193 nm; half-filled circle: population at $v=0$ estimated with surprisal analysis based on experimental data; open square: QCT calculations for reaction (1); inverted open triangle: QCT calculations for reaction (2); gray circles: QCT calculations for a weighted average of reactions (1) and (2) using the RRKM branching ratio of 0.59:0.41.

ratio of $v=0$ to $v=1$ to be 0.86 ± 0.15. The vibrational distribution of HCl normalized for $v=0-6$ is thus $(v=0)$: $(v=1)$: $(v=2)$: $(v=3)$: $(v=4)$: $(v=5)$: $(v=6)=14.1\pm6.6$:16.4 ±4.4: 18.6 ± 5.3: 18.3 ± 3.6: 15.5 ± 2.7:10.9 ±2.3: 6.3 ± 1.2, as shown in Table I and Fig. 3. The distribution does not change much when only the high-J component is taken into account, $(v=0)$:$(v=1)$:$(v=2)$:$(v=3)$:$(v=4)$:$(v=5)$:$(v=6)$ =14.3:16.6:18.7:18.2:15.0:10.6:6.6. The average vibrational energy of HCl derived from observed data is thus E_v $=86\pm5$ kJ mol^{-1}.

B. Transition states and branching of $H_2CCClCH_3$ → HCl + propyne/allene

As indicated before, the QCT calculations reported in this work were performed by using semiempirical AM1 Hamiltonians with specific reaction parameters (AM1-SRPs), obtained by fits to benchmark *ab initio* data. Among these data, we used the calculated reverse barrier heights without correction for zero-point energy (ZPE) for reactions (1) and (2), 190.8 and 182.4 kJ mol^{-1}, respectively, by Par-

TABLE I. Fitted experimental rotational temperature T_{rot}, relative population $\Sigma P_v(J)$, average rotational energy E_{rot}, vibrational population of HCl(v), average vibrational energy E_{vib}, and vibrational population of HCl(v) predicted with QCT for reactions (1) and (2).

					Vibrational population		
v	T_{rot} (K)	$\Sigma P_v(J)$ [a]	E_{rot} (kJ mol^{-1})	E_{vib} (kJ mol^{-1})	Expt.	QCT, reaction (1)	QCT, reaction (2)
0				0	~0.141 [b]	0.147	0.020
1	18 700 ± 2 300	1906	57.6	5.7[b]	0.164	0.219	0.152
2	13 900 ± 1 100	2152	48.1	12.7	0.186	0.221	0.211
3	11 800 ± 950	2092	38.6	18.2	0.183	0.176	0.203
4	11 600 ± 860	1732	30.6	19.6	0.155	0.112	0.171
5	7 100 ± 790	1220	23.4	17.0	0.109	0.067	0.114
6	9 300 ± 2 100	759	17.3	12.4	0.063	0.035	0.067
7						0.015	0.034
8						0.005	0.016
E_{av}			39.4	85.6		89	112

[a] $P_v(J)$=(relative integrated emittance)/[(instrumental response factor)(Einstein coefficient)] (a.u.).
[b] Normalized to $v=0-6$ for HCl; the population for $v=0$ is estimated.

This article is copyrighted as indicated in the article. Reuse of AIP content is subject to the terms at: http://scitation.aip.org/termsconditions. Downloaded to IP: 140.113.38.11 On: Wed, 30 Apr 2014 06:14:52

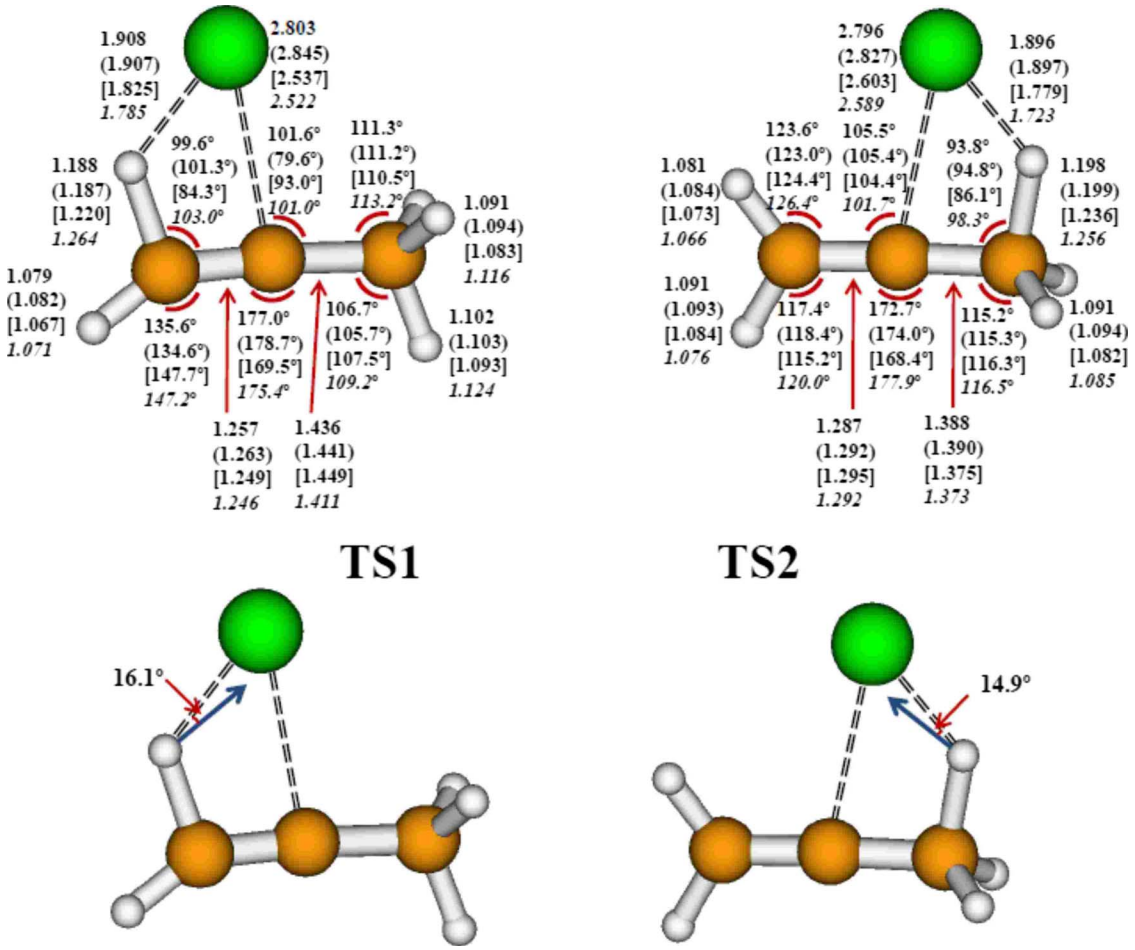

FIG. 4. (Color online) Geometries of transition states for two HCl four-center elimination channels of $H_2CCClCH_3$ producing propyne (TS1) and allene (TS2) optimized with the AM1-SRP (listed in italics) and the B3LYP/6-311G++(d,p) methods. Previous results calculated with B3LYP/6-31G(d) and MP2/6-311G(d,p) are listed in parentheses and brackets, respectively (Ref. 11). Bond lengths have unit Å. Displacement vectors and torque angles corresponding to imaginary wavenumbers predicted with B3LYP/6-311G++(d,p) are shown in the lower part.

sons *et al.*[11] at the QCISD(T)/6-311+G(d,p)//MP2/6-311G(d,p) level and the imaginary wavenumbers (1644i and 1698i cm^{-1}, respectively) at the corresponding transition states evaluated with MP2/6-311G(d,p). Our AM1-SRP Hamiltonians reproduce satisfactorily these data: 190.4 and 182.4 kJ mol^{-1} for the reverse barrier heights (without ZPE corrections) and 1646i and 1697i cm^{-1} for the imaginary wavenumbers of transition states of reactions (1) and (2), respectively. On the AM1-SRP potential-energy surface, the available energies for products (over the ZPE) are 513.0 kJ mol^{-1} for HCl+propyne and 508.8 kJ mol^{-1} for HCl+allene.

We performed calculations to optimize structures of transition states TS1 and TS2 of 2-chloropropene with the AM1-SRP and B3LYP/6-311G++(d,p) methods, as shown in Fig. 4. Geometries derived previously[11] with B3LYP/6-31G(d) and MP2/6-311G(d,p) are also listed in parentheses and brackets, respectively, for comparison; the agreements are satisfactory. The displacement vectors and torque angles corresponding to imaginary vibrational wavenumbers of TS1 and TS2 predicted with B3LYP/6-311G++(d,p) are also shown in the lower part of Fig. 4.

Vibrational wavenumbers predicted with B3LYP/6-311G++(d,p) for TS1 and TS2 are listed in Table II; values derived previously[11] with B3LYP/6-31G(d) are listed in parentheses for comparison.

Relative energies and barriers of these two molecular elimination channels derived with B3LYP/6-311G++(d,p) are shown in Fig. 5; values calculated previously[11] using QCISD(T)/6-311+G(d,p)//MP2/6-311G(d,p) and G3//B3LYP are listed in parentheses and brackets, respectively, for comparison. In addition, we include in this figure energies associated with the AM1-SRP Hamiltonians employed in the QCTs, as shown in italics. Our calculations using the B3LYP/6-311G++(d,p) method yield barriers of 242 and 237 kJ mol^{-1} for TS1 and TS2, respectively, ~15% smaller than values of 280 and 282 kJ mol^{-1} predicted using the G3//B3LYP method.[11] The AM1-SRP data reproduce the high-level quantum-chemical predictions well.

We estimated the rates of dissociation via two possible four-center elimination channels on the ground electronic surface of 2-chloropropene with the RRKM theory and calculated the density of states with the Whitten–Rabinovitch equations.[30] Using available energies of 377 and 382 kJ mol^{-1} and vibrational wavenumbers predicted for TS1 and TS2 with B3LYP/6-311G++(d,p) (Table II), we calculated rates of dissociation for reactions (1) and (2) to be

This article is copyrighted as indicated in the article. Reuse of AIP content is subject to the terms at: http://scitation.aip.org/termsconditions. Downloaded to IP: 140.113.38.11 On: Wed, 30 Apr 2014 06:14:52

TABLE II. Comparison of vibrational wavenumbers (cm^{-1}) of transition states TS1 and TS2 for elimination of HCl from $H_2CCClCH_3$ predicted with the B3LYP/6-311G++(d,p) and B3LYP/6-31G(d) methods.

	$H_2CCClCH_3$		
	Ground state	TS1	TS2
ν_1	206.9 (207.2)[a]	145.8 (145.1)[a]	182.4 (183.3)[a]
ν_2	347.0 (345.1)	166.1 (150.9)	234.0 (236.4)
ν_3	403.2 (400.2)	297.8 (306.5)	294.0 (301.6)
ν_4	452.7 (444.3)	327.8 (331.4)	341.6 (347.5)
ν_5	621.5 (627.0)	526.8 (529.5)	522.2 (524.9)
ν_6	706.2 (713.2)	547.1 (580.9)	564.9 (586.8)
ν_7	909.0 (904.1)	859.8 (880.3)	851.3 (863.8)
ν_8	927.2 (936.4)	870.7 (887.9)	902.0 (923.3)
ν_9	1016.6 (1030.0)	1008.6 (1030.8)	989.7 (1007.3)
ν_{10}	1071.6 (1085.8)	1032.1 (1069.6)	1046.5 (1062.7)
ν_{11}	1187.4 (1202.7)	1052.2 (1081.1)	1187.1 (1228.9)
ν_{12}	1407.4 (1432.6)	1378.6 (1406.1)	1296.6 (1328.7)
ν_{13}	1430.4 (1455.8)	1417.2 (1448.1)	1346.7 (1376.1)
ν_{14}	1471.4 (1498.9)	1462.6 (1487.5)	1438.2 (1464.5)
ν_{15}	1488.9 (1518.2)	1849.3 (1861.0)	1723.5 (1719.9)
ν_{16}	1699.6 (1727.7)	2017.6 (2032.0)	1966.5 (1978.1)
ν_{17}	3030.6 (3053.2)	2983.5 (3008.9)	3066.1 (3090.6)
ν_{18}	3086.7 (3112.6)	3083.7 (3108.8)	3093.6 (3129.3)
ν_{19}	3111.7 (3137.7)	3128.4 (3153.3)	3147.2 (3168.3)
ν_{20}	3150.4 (3181.6)	3251.8 (3279.9)	3232.4 (3264.4)
ν_{21}	3243.1 (3271.6)	1102*i* (1038*i*)	1116*i* (1080*i*)

[a]Previously reported values calculated with B3LYP/6-31G(d) are listed in parentheses (Ref. 11).

2.2×10^{11} and 1.5×10^{11} s^{-1}, respectively. The branching ratio for formation of propyne to that of allene, reaction (1) to reaction (2), is accordingly estimated to be 0.59:0.41. The branching ratio reported by Mueller *et al.*[10] using energies calculated with G3//B3LYP is 0.63:0.37; the small difference results from variations in calculated barriers with these two methods.

C. Quasiclassical trajectory calculations

The rotational distributions of HCl from reactions (1) and (2) predicted with QCTs are shown in Fig. 6 as symbol ○. Statistical uncertainties in rotational populations are calculated by

$$\Delta n_i = t n_i \left(\frac{n - n_i}{n_i n} \right), \tag{3}$$

in which n is the total number of trajectories, n_i is the number of trajectories leading to HCl in a particular rovibrational level, and t is the t-student value for a confidence level of 95%.[31] Both channels show similar distributions with substantial rotational excitation of HCl, having maximal populations near $J=20-27$ for various vibrational levels. According to the calculated rotational distributions, distinguishing these two channels is difficult.

The major difference between the internal distributions of HCl produced from reactions (1) and (2) lies in their vibrational distributions, which are listed in Table I and shown in Fig. 3. Statistical errors for the vibrational (and translational) distributions are negligible and so they are not reported. As illustrated in the figure, the QCT distributions have maximal populations at $v=2$. For $v=0$ and $v=1$, the HCl populations for reaction (2) shown as symbols "▽" are significantly smaller than those produced from reaction (1) shown as symbols "□". In particular, the population for $v=0$ calculated for reaction (2) is negligible. For $v>3$, the QCT calculations predict slightly less vibrational excitation for HCl produced from reaction (1) than for HCl formed via reaction (2). The QCT distributions for all HCl products obtained with a weighted sum of contributions from reactions (1) and (2), using the RRKM branching ratio of 0.59:0.41 computed in the present work, are also shown as gray circles in Fig. 3 for comparison.

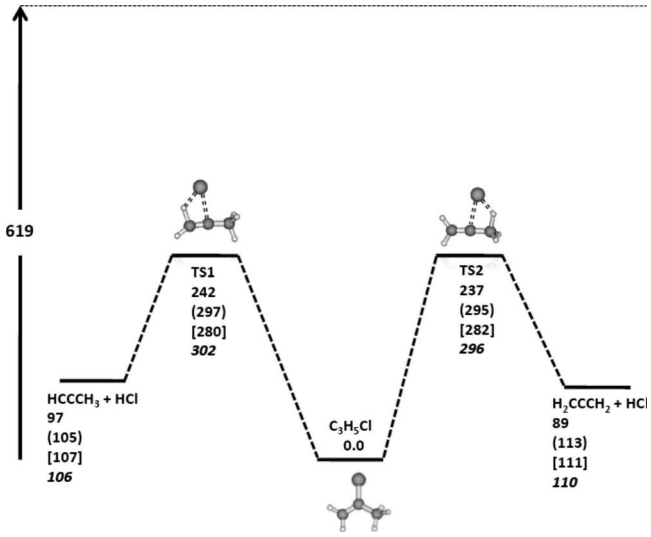

FIG. 5. Energies (in kJ mol^{-1}) of transition states (TS1 and TS2) and dissociation products relative to $H_2CCClCH_3$ predicted with the B3LYP/6-311G++(d,p) method. Those reported previously (Ref. 11) using QCISD(T) and G3//B3LYP are listed in parentheses and square brackets, respectively. Values in italic correspond to the AM1-SRP potential-energy surface. In all cases, ZPE corrections are included.

We also calculated the distributions of relative translational energy, $P(E_t)$, of reactions (1) and (2). The results are shown in Fig. 7 as continuous distributions generated by using the method of Legendre moments.[32,33] As expected, the two distributions are similar because the reverse barrier height of reaction (1), 123 kJ mol^{-1} without ZPE corrections, resembles that of reaction (2), 122 kJ mol^{-1}. Both distributions extend to ~230 kJ mol^{-1} and show maxima of ~60 kJ mol^{-1}. The predicted average translational energy for reaction (1), 83 kJ mol^{-1}, is only 8 kJ mol^{-1} greater than that for reaction (2). The QCT distribution of translational energy for the total elimination of HCl, obtained from a weighted sum of the two individual distributions using the RRKM branching ratio of 0.59:041, is shown also in the figure. For comparison purposes, we present also the experimental distribution determined by Mueller *et al.*[10] Although the total QCT distribution has a maximum at a translational energy slightly greater than the experimental one, the maximum translational energy calculated in this work agrees satisfactorily with experiment.

This article is copyrighted as indicated in the article. Reuse of AIP content is subject to the terms at: http://scitation.aip.org/termsconditions. Downloaded to IP: 140.113.38.11 On: Wed, 30 Apr 2014 06:14:52

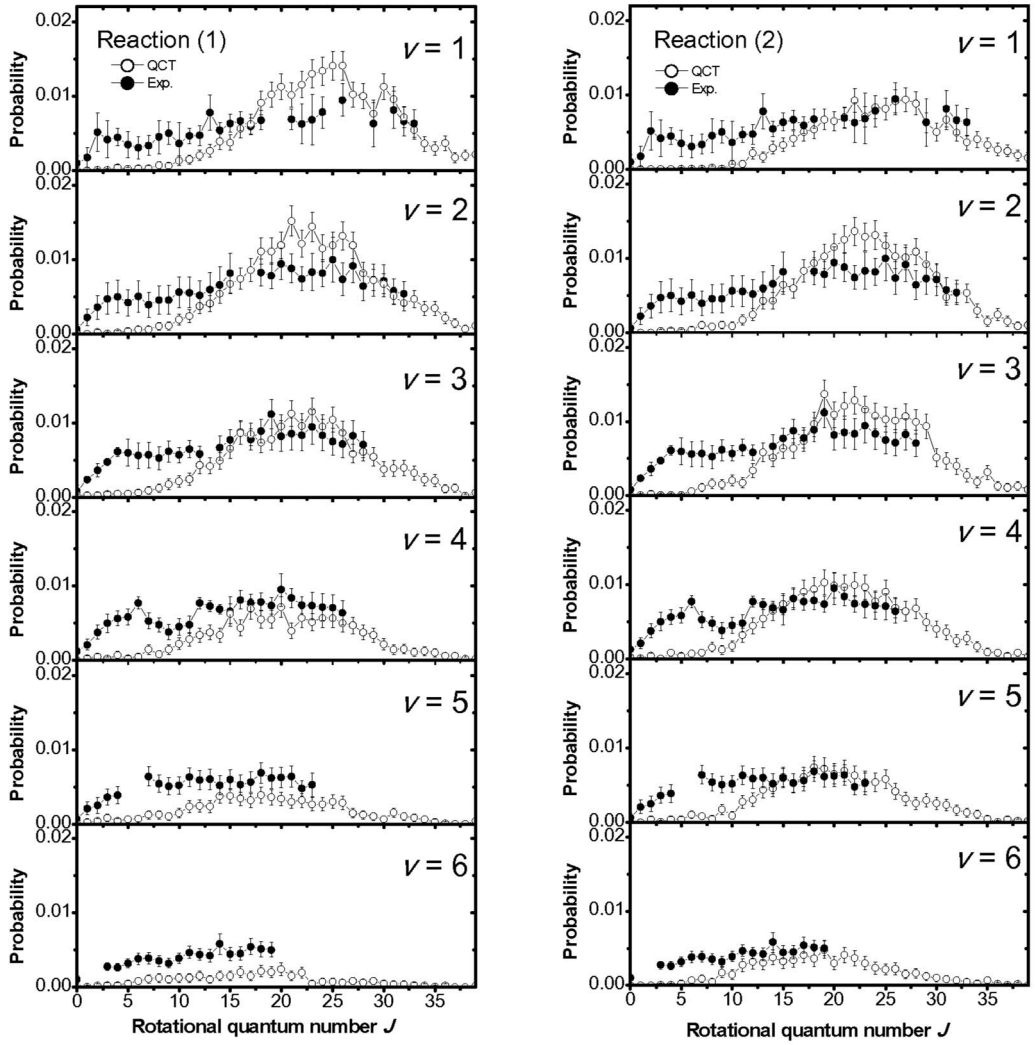

FIG. 6. Comparison of rotational distributions of HCl (v) between experiment and QCT calculations. ●: experimental data; ○: QCT calculations.

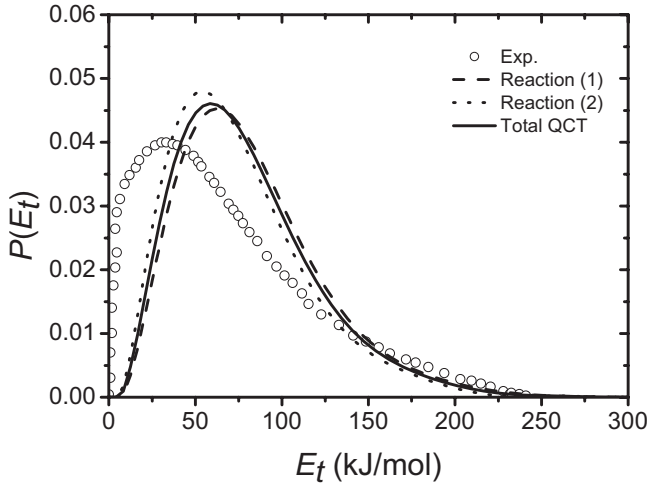

FIG. 7. Distributions of translational energy for HCl elimination calculated with classical trajectories. The total QCT distribution (solid line) is a weighted sum of the individual contributions from reactions (1) and (2), depicted by dashed and dotted lines, respectively. The experimental data (open circles) were obtained from Fig. 13 of Ref. 10 using the data digitalization program WINDIG.

V. DISCUSSION

A. Rotational energy of HCl

Our previous work[1,2,4,34,35] indicates that a revised-impulse model might satisfactorily account for the average rotational energy of HF or HCl, produced via the four-center elimination channel of several unsaturated halocompounds. Assuming that the H atom receives most available energy, we distribute the available energy between H and C atoms during bond scission, followed by calculations of translational and rotational energies of HX (X=Cl or F) according to classical mechanics. Instead of assuming that the H atom moves along the direction of the breaking bond as in the standard impulse model, we consider motions associated with the reaction coordinates described with displacement vectors associated with the imaginary vibrational wavenumber of the transition state. In the case of HCl elimination of 2-chloropropene, the direction of the H atom is assumed to follow the displacement vectors shown in the bottom part of Fig. 4. The rotational energy E_r of HCl fragment from 2-chloropropene is predicted with this modified impulse model according to the equation

This article is copyrighted as indicated in the article. Reuse of AIP content is subject to the terms at: http://scitation.aip.org/termsconditions. Downloaded to IP: 140.113.38.11 On: Wed, 30 Apr 2014 06:14:52

TABLE III. Comparison of total available energy E_{ava}, exit barrier E_{exit}, H–Cl length R_{HCl}, and torque angle α of HCl-elimination transition states, observed average rotational energy E_r and average vibrational energy E_v, and those predicted with QCT (AM1-SRP) calculations.

	$CH_2CHCl \rightarrow HCl + C_2H_2$			$H_2CCClCH_3 \rightarrow HCl + HCCCH_3H_2CCCH_2$		
Reaction	Three center	Four center	Total	Reaction(1)	Reaction(2)	Total
E_{ava} (kJ mol^{-1})	515	515		522	530	
E_{exit} (kJ mol^{-1})	185	220		145	148	
R_{HCl} (Å)	1.40	1.80		1.91	1.90	
α (deg)	24.0	4.3		16.1	14.9	
E_r (kJ mol^{-1}) (impulse)[a]	27	1.1		11.2	9.8	
E_r(expt.) (kJ mol^{-1})			44 ± 6			$39 \pm {}^{11}_{3}$
E_r (QCT) (kJ mol^{-1})	44	71	49[b]	66	68	67[c]
E_v(expt.) (kJ mol^{-1})			75 ± 3			86 ± 5 [d]
E_v (QCT) (kJ mol^{-1})	39	122	56[b]	89 (86)[d]	112 (104)[d]	98[c](93)[d]
Reference		1 and 7–9			This work	

[a]Assuming the motion of H atom to occur along the displacement vector corresponding to the imaginary mode of the transition state; see text.
[b]Assuming a 4:1 ratio for the three-center to four-center elimination channels.
[c]Assuming a 0.59:0.41 ratio for reactions (1) and (2).
[d]Average vibrational energy if only $v=0-6$ levels are counted (as experimentally observed).

$$E_r = [m_{Cl}m_C/(m_H + m_{Cl})(m_H + m_C)]E_{avail} \sin^2 \alpha, \quad (4)$$

in which E_{avail} is the available energy (reverse barrier) and α is the torque angle between the direction of motion of H and that of the H–Cl bond. With exit barriers of 145 and 148 kJ mol^{-1} and $\alpha = 16.1°$ and 14.9° predicted for TS1 and TS2, respectively, rotational energies of 11.1 and 9.8 kJ mol^{-1} are predicted, much smaller than the experimental observation of $39 \pm {}^{11}_{3}$ kJ mol^{-1}. The modified impulse model is hence inapplicable to this case.

One possible reason for the inadequacy of the modified impulse model to this system might be related to the "tightness" of the transition state. The modified impulse model takes into account mainly the motion of the H atom near the transition state region; hence it is expected to be valid when the transition state is "loose," which is the case for the four-center elimination of fluorobenzene,[34] fluorotoluene[35] (both with a C–H bond of ~1.60 Å), and CF_2CHCl (with a C–H bond of ~1.41 Å).[4] In contrast, the C–H bond length is ~1.19 Å for the transition states of reactions (1) and (2); the impulse resulted from the dissociation of the C–H bond might increase the effective torque angle of the H atom toward Cl, hence increase the rotational excitation of the HCl product.

The observed rotational distributions of the high-J component fit qualitatively with the distributions of both channels obtained with QCTs, as compared in Fig. 6, but the QCT calculations predict negligible populations for states at small J. The average rotational energies computed by trajectories, 66 and 68 kJ mol^{-1} for reactions (1) and (2), respectively, are significantly greater than the observed value of $39 \pm {}^{11}_{3}$ kJ mol^{-1} (see Table III) even when the upper limit (50 kJ mol^{-1}) of the experimental value is compared. As described in Sec. IV A, this upper limit is derived on counting all levels below the observed level with the highest energy even if they were unobserved; a Boltzmann distribution was assumed. A possible explanation for this discrepancy is suggested in Sec. V C.

B. Vibrational energy of HCl

The average vibrational energy of 86 ± 5 kJ mol^{-1} for HCl implies that a moderate fraction of available energy is partitioned into HCl, with $f_v \cong 0.16 \pm 0.01$. The partition of vibrational energy depends on the deviation of the distance between two bond-forming atoms at the transition state from the equilibrium bond length. Predicted distances between H and Cl for TS1 and TS2 in dissociation of 2-chloropropene are 1.91 and 1.90 Å, respectively. Because the equilibrium bond distance of HCl is 1.275 Å,[36] the vibrational distribution of HCl produced via the four-center elimination is expected to be highly excited, consistent with the inverted vibrational distribution predicted with calculations and also observed in this work.

Figure 3 shows a comparison between the observed relative vibrational populations of HCl with those calculated by QCTs. The observed vibrational distribution (symbol ●) shows more excitation than that predicted for reaction (1) with QCT (symbol □) but less excitation than that predicted for reaction (2) with QCT (symbol ▽). The experimental vibrational distribution only agrees qualitatively with the QCT-predicted distributions for both reactions, but it agrees better with the total QCT distribution (shown as gray circles), obtained as a weighted sum of contributions from reactions (1) and (2). Both distributions show that the most probable vibrational state of the HCl photofragment corresponds to $v=2$. However, because predicted vibrational distributions are not very different, it is difficult to derive the branching ratio based on current data.

If only $v=0-6$ is counted, the average vibrational energy for HCl from reactions (1) and (2) is predicted with QCT to be 86 and 104 kJ mol^{-1}, respectively; an average energy of 93 kJ mol^{-1} is derived for the total reaction obtained as a weighted sum of contributions from reactions (1) and (2), in agreement with the observed average vibrational energy of 86 ± 5 kJ mol^{-1} for HCl from photolysis of 2-chloropropene.

This article is copyrighted as indicated in the article. Reuse of AIP content is subject to the terms at: http://scitation.aip.org/termsconditions. Downloaded to IP: 140.113.38.11 On: Wed, 30 Apr 2014 06:14:52

Finally, we noticed that the average vibrational energy of HCl calculated for reaction (2), i.e., allene formation, is 23 kJ mol^{-1} greater than that predicted for reaction (1). This appears to be quite surprising because both channels have almost the same available energy and exit barrier. In order to get some insights into the origin of this difference, for each channel we run a single trajectory, starting at the transition state with no vibrational energy (1 kJ mol^{-1} was added to the reaction coordinate to facilitate initial propagation of the trajectory toward products). We were interested in analyzing the role of the exit channel, excluding vibrational effects, in the vibration of HCl product. The use of a single trajectory to study product energy partitioning in unimolecular reactions, and particularly mass effects in halogenated alkanes, was discussed by Sun *et al.*[37] Our single trajectory calculations yield vibrational energies of 65 and 90 kJ mol^{-1} for HCl produced from reactions (1) and (2), respectively, which follow the same trend predicted at 193 nm. These results suggest that subtle details in the topology of the exit channel may have a significant influence on product energy partitioning.

C. Comparison with photolysis of vinyl chloride

The fact that we observed substantial rotational excitation of HCl upon photolysis of 2-chloropropene at 193 nm via four-center elimination indicates that our postulate of previously observed low-J component of HCl product, with $E_r = 3.8 \pm 0.3$ kJ mol^{-1}, corresponding to the four-center elimination channel of vinyl chloride upon photolysis at 193 nm[1] might be in error; QCT calculations also indicate that both three-center and four-center HCl-elimination channels of vinyl chloride yield rotationally excited HCl, with the latter yielding HCl with slightly higher average rotational energy. As discussed in Sec. V A, the modified impulse model underestimates the rotational excitation of HCl from 2-chloropropene; similar situation is observed for photolysis of vinyl chloride.

The internal energies observed for HCl from vinyl chloride and 2-chloropropene are compared with those calculated with the modified impulse model and the QCT method in Table III. For the photolysis of vinyl chloride, a ratio of 4:1 for the three-center to four-center HCl elimination channels is assumed in direct MP2/6-31G(d,p) and AM1-SRP trajectory calculations to derive average rotational energies of $E_r = 39$ and 49 kJ mol^{-1}, respectively. For the four-center elimination of HCl from vinyl chloride, $E_r = 85$ and 71 kJ mol^{-1}, based on QCT calculations using MP2/6-31G(d,p) and AM1-SRP methods, respectively. The latter value is similar to the average rotational energies predicted with our QCT calculations for four-center HCl elimination from 2-chloropropene via reactions (1) and (2), 66 and 68 kJ mol^{-1}, respectively. The trajectory simulations predict that the average rotational energy of HCl in the photodissociation of 2-chloropropene, with contributions from two four-center elimination channels, is greater than that of HCl in the photodissociation of vinyl chloride, with contributions of three-center and four-center elimination channels, but the experimental results show an opposite trend.

To suggest a possible reason for this disagreement, one must bear in mind the fundamental approximations inherent to our QCT calculations. First, we use classical dynamics, but we expect classical dynamics to be reliable as comparisons with quantum dynamics indicate that classical dynamics affords accurate results for direct processes such as the motion down of a potential-energy barrier provided that trajectories are initialized with appropriate quasiclassical conditions.[38] Second, the trajectories are integrated using semiempirical AM1-SRP Hamiltonians, which might model inaccurately the exit channels of reactions (1) and (2). Although methods of this type provide, in general, acceptable results for qualitative and even semiquantitative purposes, there might arise instances in which subtle features of the potential-energy surface have a significant role in the dynamics. Third, initial conditions are imposed through a microcanonical sampling of molecular states at the barrier; internal conversion from the electronic excited state is hence followed by a rapid redistribution of the intramolecular vibrational energy, so that the dynamics at the reactant phase space is ergodic. Internal conversion might, however, concentrate most internal energy in a few vibrational degrees of freedom, and, because the excitation energy is large, dissociation on the ground state might occur on a short time scale, before complete randomization of the vibrational energy; this has been defined in the literature as apparent non-RRKM behavior.[39] Moreover, conical intersections between excited and ground electronic states might promote reaction pathways that have not been considered in this study. In fact, multiconfigurational and multireference *ab initio* calculations on vinyl fluoride[40] and difluoroethylenes[41] have shown S_0/S_1 conical intersections associated with hydrogen migration, which might play a significant role in the photodissociation of these systems through increasing the probability of this process.

The average vibrational energy of HCl, 86 ± 5 kJ mol^{-1}, observed on photolysis of 2-chloropropene at 193 nm is slightly larger than that from vinyl chloride, 74 ± 3 kJ mol^{-1}. This order is reasonable because predicted bond distances of transition states, ~1.90 Å for both reactions (1) and (2), are greater than that for the corresponding transition state of vinyl chloride, 1.80 Å. Although the observed average vibrational energy of 86 ± 5 kJ mol^{-1} for HCl from photolysis of 2-chloropropene appears to be slightly smaller than the weighted total vibrational energy of 98 kJ mol^{-1} predicted with QCT, it agrees reasonably well with the average value of 93 kJ mol^{-1} if only $v=0-6$ states are taken into account. In contrast, the experimental value of 74 ± 3 kJ mol^{-1} for average vibrational energy of HCl from vinyl chloride is greater than the weighted total vibrational energy of 56 kJ mol^{-1} predicted with QCT.[8,9] Averaged vibrational energies of 122 and 39 kJ mol^{-1} were predicted with QCT for HCl produced from four-center and three-center elimination channels of vinyl chloride, respectively; a small variation in the branching ratio affects the weighted average value significantly.

Finally, it is interesting to compare the $P(E_t)$ distributions calculated in this work with those predicted for four-center elimination from vinyl chloride in previous QCT

This article is copyrighted as indicated in the article. Reuse of AIP content is subject to the terms at: http://scitation.aip.org/termsconditions. Downloaded to IP: 140.113.38.11 On: Wed, 30 Apr 2014 06:14:52

studies.[8,9] The $P(E_t)$ distributions for reactions (1) and (2) have maxima around 60 kJ mol^{-1} and average values around 80 kJ mol^{-1}. The $P(E_t)$ distributions for HCl production from photolysis of vinyl chloride, afforded by both MP2/6-31G(d,p) and AM1-SRP trajectories, peak close to 135 kJ mol^{-1} and have average values of about 150 kJ mol^{-1}, respectively. The reverse barrier height in four-center elimination from vinyl chloride is approximately 30 kJ mol^{-1} greater than those in 2-chloropropene, which facilitates more transfer of energy to product translation. However, this difference of 30 kJ mol^{-1} between the reverse barrier heights is about half of the difference of the peak energies, and so there seems to be other reasons for the much larger translational energy release in four-center elimination from vinyl chloride. To clarify this, we performed additional trajectory calculations. In order to assess the role of the exit barrier in product translation, we first ran for each case a single trajectory with no vibrational energy at the transition state, as mentioned before. Second, we carried out QCT calculations with no excess energy at the barrier (i.e., only ZPE). The former calculations showed that in vinyl chloride, 38% of the energy provided by the exit barrier goes to translation (83 kJ mol^{-1}), whereas in reactions (1) and (2) of 2-chloropropene, the percentages are 25% and 19%, and the relative translational energies are 49 and 39 kJ mol^{-1}, respectively. Therefore, both the height of the reverse barrier and the percentage of the available energy that goes to translation are more important for four-center elimination from vinyl chloride, leading to more translational energy disposal in this system.

On the other hand, for the four-center elimination from vinyl chloride, the QCT calculations with only the ZPE in the normal modes predicted a distribution peaking at ~90 kJ mol^{-1}, with an average energy of 96 kJ mol^{-1}. For reactions (1) and (2), the distributions peak at ~50 and ~42 kJ mol^{-1}, respectively, and have average energies of 53 and 44 kJ mol^{-1}, respectively. These values, especially the most probable translational energies, are slightly higher than the translational energies predicted by the single trajectory calculations. It is also apparent that, when ZPE is included, the translational energy release increases somewhat more in four-center elimination from vinyl chloride than does in reactions (1) and (2), which suggests that coupling between vibration (transitional vibrational modes are preferentially involved) and product translation is more significant in the former system. For excitation at 193 nm, both the most probable and the average translational energy increase more markedly (in absolute value) in four-center elimination from vinyl chloride than from 2-chloropropene. Again, this may be due to stronger couplings between transitional vibrational modes and relative translation in vinyl chloride, as well as to the fact that in 2-chloropropene there are more degrees of freedom among which the excess energy is distributed.

VI. CONCLUSION

Rotationally resolved emission from HCl up to $v=6$ is observed upon photolysis of 2-chloropropene at 193 nm. HCl might be produced from both four-center elimination channels with propyne or allene as associated fragments, respectively; these two reactions were predicted to have a branching ratio of 0.59:0.41 according to RRKM calculations. The observed rotational distributions fit qualitatively with the distributions of both channels obtained with QCTs, but the QCT calculations predict negligible populations for states at small J. The observed vibrational distribution agrees satisfactorily with the total QCT distribution obtained as a weighted sum of contributions from both four-center elimination channels. The observed average rotational energy of $39\pm^{11}_{3}$ kJ mol^{-1} is slightly smaller than the value of 47 ± 2 kJ mol^{-1} derived for HCl on photolysis of vinyl chloride, but the average vibrational energy of 86 ± 5 kJ mol^{-1} is slightly greater than the value of 74 ± 3 kJ mol^{-1} derived for HCl on photolysis of vinyl chloride; the latter is consistent with a more elongated H–Cl bond in the transition states for 2-chloropropene→HCl+propyne or allene than for vinylchloride→HCl+acetylene. The modified impulse model considering displacement vectors of transition states during bond scission fails to predict satisfactorily the rotational distributions of HCl produced from the four-center elimination channels of vinyl chloride and 2-chloropropene.

ACKNOWLEDGMENTS

The National Science Council of Taiwan (Grant No. NSC96-2113-M009-025) and the Ministry of Education MOE-ATU project supported this work. We thank the National Center for High-Performance Computing of Taiwan for computer time. M.P.-P., E.M.-N., and S.A.V. thank "Xunta de Galicia" ("Axuda para Consolidación e Estruturación de unidades de investigación competitivas do Sistema Universitario de Galicia, Xunta de Galicia 2007/050, cofinanciada polo FEDER 2007-2013") for financial support.

[1] S.-R. Lin, S.-C. Lin, Y.-C. Lee, Y.-C. Chou, I.-C. Chen, and Y.-P. Lee, J. Chem. Phys. **114**, 160 (2001).
[2] S.-R. Lin, S.-C. Lin, Y.-C. Lee, Y.-C. Chou, I.-C. Chen, and Y.-P. Lee, J. Chem. Phys. **114**, 7396 (2001).
[3] D. A. Blank, W. Sun, A. G. Suits, Y. T. Lee, S. W. North, and G. E. Hall, J. Chem. Phys. **108**, 5414 (1998).
[4] C.-Y. Wu, C.-Y. Chung, Y.-C. Lee, and Y.-P. Lee, J. Chem. Phys. **117**, 9785 (2002).
[5] C.-Y. Wu, Y.-P. Lee, J. F. Ogilvie, and N. S. Wang, J. Phys. Chem. A **107**, 2389 (2003).
[6] C.-Y. Wu, Y.-P. Lee, and N. S. Wang, J. Chem. Phys. **120**, 6957 (2004).
[7] M. Bahou and Y.-P. Lee, Aust. J. Chem. **57**, 1161 (2004).
[8] E. Martínez-Núñez, A. Fernández-Ramos, S. A. Vázquez, F. J. Aoiz, and L. Bañares, J. Phys. Chem. A **107**, 7611 (2003).
[9] E. Martínez-Núñez, S. A. Vázquez, F. J. Aoiz, L. Bañares, and J. F. Castillo, Chem. Phys. Lett. **386**, 225 (2004).
[10] J. A. Mueller, B. F. Parsons, L. J. Butler, F. Qi, O. Sorkhabi, and A. G. Suits, J. Chem. Phys. **114**, 4505 (2001).
[11] B. F. Parsons, L. J. Butler, and B. Ruscic, Mol. Phys. **100**, 865 (2002).
[12] P.-S. Yeh, G.-H. Leu, Y.-P. Lee, and I.-C. Chen, J. Chem. Phys. **103**, 4879 (1995).
[13] S.-R. Lin and Y.-P. Lee, J. Chem. Phys. **111**, 9233 (1999).
[14] C. Doubleday, K. Bolton, G. H. Peslherbe, and W. L. Hase, J. Am. Chem. Soc. **118**, 9922 (1996).
[15] K. Bolton, W. L. Hase, and G. H. Peslherbe, *Modern Methods for Multidimensional Dynamics in Chemistry* (World Scientific, Singapore, 1998).
[16] J. González-Vázquez, E. Martínez-Núñez, A. Fernández-Ramos, and S. A. Vázquez, J. Phys. Chem. A **107**, 1398 (2003).
[17] S. A. Vázquez, F. J. Aoiz, L. Bañares, J. Santamaría, E. Martínez-Núñez, and A. Fernández-Ramos, J. Chem. Phys. **118**, 6941 (2003).

This article is copyrighted as indicated in the article. Reuse of AIP content is subject to the terms at: http://scitation.aip.org/termsconditions. Downloaded to IP: 140.113.38.11 On: Wed, 30 Apr 2014 06:14:52

[18] E. Martínez-Núñez and S. A. Vazquez, Chem. Phys. Lett. **425**, 22 (2006).
[19] A. D. Becke, J. Chem. Phys. **98**, 5648 (1993).
[20] C. Lee, W. Yang, and R. G. Parr, Phys. Rev. B **37**, 785 (1988).
[21] M. J. Frisch, G. W. Trucks, H. B. Schlegel *et al.*, GAUSSIAN 03, Revision A.1, Gaussian Inc., Pittsburgh, PA, 2003.
[22] D. L. Thompson, GENDYN program.
[23] J. P. P. Stewart, MOPAC7.0, a general molecular orbital package (QCPE p. 455, 1993); J. P. P. Stewart, J. Comput. Chem. **10**, 209 (1989).
[24] A. Einstein, Verh. Dtsch. Phys. Ges. **19**, 82 (1917).
[25] M. L. Brillouin, J. Phys. Radium **7**, 353 (1926).
[26] J. B. Keller, Ann. Phys. (N.Y.) **4**, 180 (1958).
[27] E. Arunan, D. S. Setser, and J. F. Ogilvie, J. Chem. Phys. **97**, 1734 (1992).
[28] J. A. Coxon and U. K. Roychowdhury, Can. J. Phys. **63**, 1485 (1985).
[29] E. Arunan, D. W. Setser, and J. F. Ogilvie, J. Chem. Phys. **97**, 1734 (1992).
[30] K. A. Holbrook, M. J. Pilling, and S. H. Robertson, *Unimolecular Reactions*, 2nd ed. (Chichester, New York, 1996).
[31] G. H. Peslherbe and W. L. Hase, J. Chem. Phys. **101**, 8535 (1994).
[32] F. J. Aoiz, V. J. Herrero, and V. Sáez Rábanos, J. Chem. Phys. **97**, 7423 (1992).
[33] F. J. Aoiz, L. Bañares, and V. J. Herrero, J. Chem. Soc., Faraday Trans. **94**, 2483 (1998).
[34] C.-Y. Wu, Y.-J. Wu, and Y.-P. Lee, J. Chem. Phys. **121**, 8792 (2004).
[35] S.-K. Yang, S.-Y. Liu, H.-F. Chen, and Y.-P. Lee, J. Chem. Phys. **123**, 224304 (2005).
[36] K. P. Huber and G. Herzberg, *Constants of Diatomic Molecules* (van Nostrand, Princeton, 1979).
[37] L. Sun, K. Park, K. Song, D. W. Setser, and W. L. Hase, J. Chem. Phys. **124**, 064313 (2006).
[38] A. Untch, R. Schinke, R. Cotting, and J. R. Huber, J. Chem. Phys. **99**, 9553 (1993).
[39] D. L. Bunker and W. L. Hase, J. Chem. Phys. **59**, 4621 (1973).
[40] M. Barbatti, A. J. A. Aquino, and H. Lischka, J. Phys. Chem. A **109**, 5168 (2005).
[41] J. González-Vázquez and L. González, Chem. Phys. **349**, 287 (2008).

This article is copyrighted as indicated in the article. Reuse of AIP content is subject to the terms at: http://scitation.aip.org/termsconditions. Downloaded to IP: 140.113.38.11 On: Wed, 30 Apr 2014 06:14:52